Korean J. Chem. Eng., **31**(9), 1632-1640 (2014)
DOI: 10.1007/s11814-014-0118-z

pISSN: 0256-1115
eISSN: 1975-7220

Supercritical extraction of essential oil from *Echium amoenum* seed : Experimental, modeling and genetic algorithm parameter estimation

Seyyed Mohammad Ghoreishi† and Ehsan Bataghva

Department of Chemical Engineering, Isfahan University of Technology, Isfahan 84156-83111, Iran
(*Received 22 October 2013 • accepted 20 April 2014*)

Abstract−Mathematical modeling of supercritical CO_2 extraction of essential oil from *Echium amoenum* seed was carried out. The effect of process variables such as pressure (15, 20, 25 and 30 MPa), temperature (313, 318, 323 and 328 K) and CO_2 flow rate (0.6, 0.9, 1.2 and 1.5 ml/min) on the recovery of essential oil extraction was investigated in a series of experiments conducted in a laboratory scale apparatus. The chemical composition of recovered essential oil (fatty acids) was analyzed by GC-FID. The mathematical model was developed utilizing diffusion-controlled regime in the pore and film mass transfer resistances with axial dispersion of the mobile phase at dynamic conditions. Henry's law was used to describe the equilibrium state of solid and pore fluid phases. The obtained mass transfer equations for the mobile and stationary phases were solved using the numerical explicit method of line, and the modeling predictions of oil extraction recovery were validated via comparison with experimental data. Genetic algorithm (GA) was applied to estimate the optimum value of the Henry constant. Finally, applying the validated model the extraction recovery was investigated as a function of effective variables such as dynamic extraction time and supercritical fluid temperature, pressure and flow rate. A set of optimal operating conditions were determined via modeling parametric analysis to achieve the objective function of maximum recovery.

Keywords: Supercritical Fluid Extraction, Modeling, *Echium amoenum* Seed, Genetic Algorithm

INTRODUCTION

Echium amoenum or *Boraginace* is an indigenous Iranian plant that has long been used in traditional medicine. Petals of *E. amoenum* have been advocated for a variety of effects such as demulcent, anti-inflammatory and analgesic, especially for common cold, anxiolytic, sedative and other psychiatric symptoms including obsession in folk medicine of Iran [1]. The oil of Boraginace seed is the source of polyunsaturated fatty acids such as γ-linolenic acid (GLA) and stearidonic acid (SDA) that have been shown to selectively kill tumor cells without harming normal cells [2]. But in chemotherapy, which is commonly used for cancer treatment via application of a number of different anticancer drugs, a number of the body's normal, non-cancerous cells also divide rapidly and are harmed [3]. Therefore, production of GLA and SDA from natural resources is considered to be an important research area in the pharmaceutical and medicinal industry.

In the field of extraction processes, using supercritical fluids such as CO_2 overcomes many drawbacks linked to the use of liquid organic solvents such as liquid hexane. Solvents commonly used present problems of toxicity and residual content in the final products after extraction. In addition to toxicity, there is also the problem of security during storage due to flammability. In this context, supercritical fluid extraction (SFE), especially supercritical carbon dioxide (SC-CO_2) extraction, has attracted attention as an efficient extraction method in the last two decades, as its advantages include being non-explosive, non-toxic, non-solvent residual and its availability in high purity with low cost [4].

Experimental concentration profiles of solute in both solid and fluid phases through the fixed bed cannot be easily obtained during the SFE extraction process. Continuous sampling under high pressures is difficult, expensive, time-consuming and not always possible. Nevertheless, these concentration profiles can be predicted by using SFE models once their parameters have been properly fit to the experimental data. Thus, a validated model allows one to predict the SFE behavior before carrying out the experiment, which reduces time and targets the experiments with definitive criteria [5]. In some previous studies, the advances and applications of kinetic models for describing supercritical fluid extraction from various solid matrices were presented [6,7]. The available mathematical models to describe the extraction of solutes from solid matrices using supercritical fluids are classified in four main groups: empirical models, models based on heat transfer analogies, shrinking core model and models based on differential mass balance. The modeling advantage of the first group such as Bernardo-Gil and Casquilho [8] and Mongkholkhajornsilp et al. [9] is their simplicity, but the disadvantages are that the corresponding parameters have no physical significance and being unsuitable for scaling up. The models based on heat transfer analogies (Gaspar et al. [10] and Reverchon and Osseo [11]) assumed one adjustable parameter (effective pore diffusivity), and only the internal mass transfer resistance gave little information about the early stage of the extraction and neglected the rate limitation related to the solubility/phase equilibrium. Therefore, considerable deviations were observed between modeling prediction and experimental measurements. The third type, the shrinking core model, assumed that the solute concentration within the core to be con-

†To whom correspondence should be addressed.
E-mail: ghoreshi@cc.iut.ac.ir

stant throughout the extraction process, neglected the axial dispersion and considered two adjustable parameters (effective pore diffusivity, external mass transfer coefficient). Salgın et al. [12] satisfactorily described the experimental results of the sunflower oil extraction via this model. The fourth group of models has stronger physical significance by considering the characteristics of the plant matrix (particle size and the bed porosity) and includes mass transfer coefficients in fluid and solid phases or in just one phase. These models are based on differential mass balances and reflect the mechanisms behind the extraction process (equilibrium relationships and mass transfer mechanisms). Some reported studies for this group are canola oil seed [13], clove bud volatile oil [14] and rose and tuberose volatile oils [15] by assuming that the external mass transfer resistance controls the extraction. Some other researches such as Reis-Vasco et al. [16] described the diffusion inside the particle as the controlling step for pennyroyal volatile oil. Some other modeling studies have also been reported such as the extraction of the oils from olive leaves [17], grapes [18], sea buckthorn [19], almond [20] and fennel [21] by considering the mass transfer resistances in fluid and solid phases. For example, based on the broken and intact cell walls idea, Sovov [18] proposed a model in which the solute is divided in two fractions: the easily accessible solute and the hardly accessible solute. During SFE process, for each particle, all the easily accessible solute is extracted before the hardly accessible solute begins to be removed. So, the SFE process can be divided in three steps: in the first step there is easily accessible solute in every particle of the extraction bed; in the second step, the easily accessible solute is gradually depleted from the inlet to the outlet of the bed; and in the third step there is only hardly accessible solute.

In the present study, supercritical CO_2 extraction of essential oil from *E. amoenum* seed was accomplished at four different temperatures (313, 318, 323 and 328 K), four different pressures (15, 20, 25 and 30 MPa) and four different flow rates (0.6, 0.9, 1.2 and 1.5 ml/min). The parametric analysis (pressure, temperature, flow rate of supercritical carbon dioxide and dynamic extraction time) was studied via a validated mathematical model. In the developed model, GA was used to obtain equilibrium parameter (Henry constant). The obtained results of experimental extraction of essential fatty acids were used for model validation. Furthermore, the objective function of maximum extraction recovery was investigated as a function of effective variables via the validated model parametric analysis which led to the determination of a set of optimal operating conditions.

EXPERIMENTAL

1. Materials

The *E. amoenum* seed was obtained from Isfahan agricultural research center. Fatty acid methyl ester (FAME) standards were purchased from Sigma. Petroleum ether and trioctylamine (99.6%, Merck) were used as the Soxhlet extraction solvent and the internal standard for the gas chromatography-flame ionization detector (GC-FID) calibration analysis, respectively. The *E. amoenum* seeds were ground into small particle size and sieved (mesh size 35; 0.5 mm). Industrial grade carbon dioxide (≥99%, Zamzam) was used as the supercritical fluid.

2. Oil Extraction by Soxhlet Method

To compare the yield of conventional solvent extraction with that of the SFE method, a Soxhlet apparatus with petroleum ether (solvent) was used. Total oil content of the *E. amoenum* seed was determined to be 24.0 wt%. The oil yield was estimated gravimetrically [17].

3. Supercritical CO_2 Extraction

A schematic flow diagram of the experimental setup is shown in Fig. 1. To increase the purity of the CO_2, which is stored in a CO_2 cylinder (1), it is passed through a column of molecular sieve beads (2). Then, CO_2 is cooled to 0 °C in a cooler (LAUDA ecoline) (3), and subsequently charged by a feed pump (Jasco) (4). A valve (5) is placed at the effluent of the pump, and thus, the CO_2 stream is easily controlled and saved properly for further use. Carbon dioxide is heated before entering the extraction column by using a coil preheater (6) that is placed in an oven (Jasco) (10). The system pres-

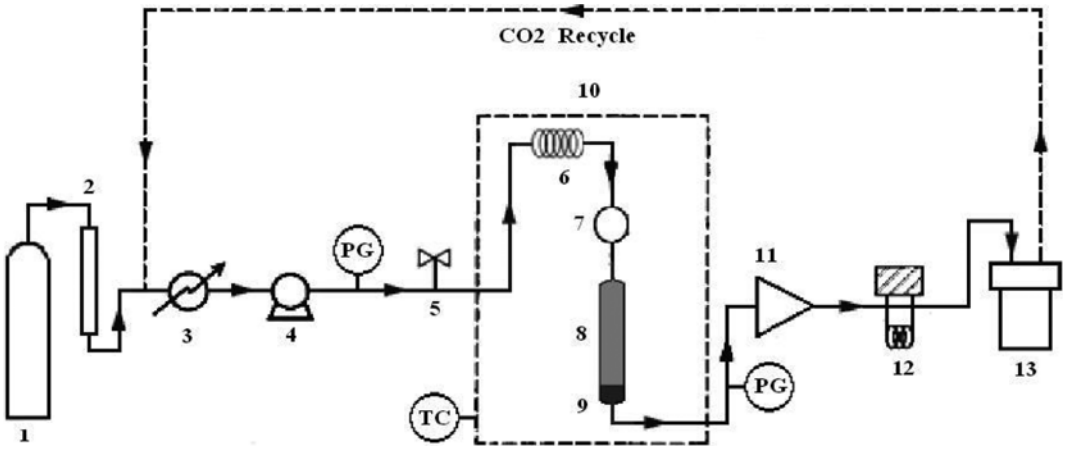

Fig. 1. The experimental setup for the supercritical extraction system.

1. CO_2 cylinder
2. Molecular sieve column
3. Cooler
4. HPLC pump
5. Valve
6. Coil preheater
7. Injection valve
8. Extraction column
9. Cotton wool filter
10. Oven
11. Back pressure regulator
12. Restrictor heater
13. Collection vessel

PG. Pressure gauge
TC. Temperature controller

sure is controlled and monitored by a back pressure regulator (Jasco) (11) and a high-pressure pump. At the effluent of the back pressure regulator, a restrictor heater (12) increases the temperature of the exit solution stream to 80 °C to prevent a possible serious safety problem caused by the Joule-Thompson effect that may result in freezing of the carbon dioxide. The stainless steel extraction column (diameter of 0.01 m and length of 0.13 m) (8) fitted with cotton wool (9) at the effluent is manually charged with *E. amoenum* seed and glass beads with a mesh size of 35 (0.5 mm) in a ratio of 40-60% (w/w), respectively. The extraction procedure consisted of static (batch mode) and dynamic periods (discharge mode) of extraction. First, carbon dioxide is charged into the extraction column while the back pressure regulator is set at the selected operating pressure and the desired temperature is obtained via the constant temperature bath and preheater. After reaching the appropriate pressure and temperature in the column, the pump is turned off and isolated with a shut-off valve. Subsequently, a period of static extraction time is allowed for SC-CO_2 to dissolve the oil. After 25 min of static extraction, the dynamic extraction with constant volumetric flow rate of CO_2 is started for different dynamic times. The dissolved oil is discharged from the column, trapped, and collected via supercritical fluid expansion in the test tube at −5 °C. The essential oil (golden-yellow color) contained in the extracted samples was kept in the refrigerator for further GC-FID analysis. The oil extraction recovery via SFE was calculated using the following Eq.:

$$\text{Oil extraction recovery (\%)} = \frac{\text{mass of extracted oil}}{\text{mass of soxhlet extracted oil}} \times 1000 \quad (1)$$

The extracted oil with Soxhlet process was considered as the total oil content.

4. Analysis of *E. amoenum* Seed Oil

Oil composition (main fatty acids) was identified by GC-FID (Agilent Technologies, 6890N) equipped with a capillary column (HP88; 100 m×0.25 mm I.D., 0.2 μm film thickness). Prior to injection, the extracted oil was converted to its FAMEs via esterification reaction according to the method described by Kim et al. [22]. The oven temperature was initially set at 150 °C, raised to 190 °C at rate of 5 °C/min and held constant for 2 min. The temperature was finally raised to 240 °C at rate of 5 °C/min and kept constant for 8 min. The sample compartment (1 μL) was flushed through with carrier gas (nitrogen) at rate of 1.5 ml/min. The injector and detector temperatures were 250 and 260 °C, respectively. The peaks of different components were identified by comparison with known methyl ester standards and trioctylamine was used as internal standard.

MATHEMATICAL MODELING

1. General Assumptions

The following criteria were assumed in this study: (1) The system was isothermal and isobaric and the constant physical properties of SC-CO_2 were considered; (2) The extraction model was expressed as an irreversible desorption process; (3) Radial dispersion was neglected because of the packed bed geometry (small column diameter); since the spreading of the concentration front in a chromatographic system is due entirely to the axial dispersion and bulk flow effects, the radial dispersion is thus insignificant and can be omitted; (4) A single pseudo-component was considered because components in the essential oil behave very similarly in terms of mass transfer phenomenon and furthermore the dominant fatty acid in the *E. amoenum* seed oil is α-linolenic acid (ALA); (5) All particles were considered to be spherical, uniformly wetted with constant porosity and essential oil was uniformly distributed throughout the particles; (6) The solvent flow rate was constant along the bed and uniformly distributed; and (7) A linear equilibrium relationship using Henry constant was applied.

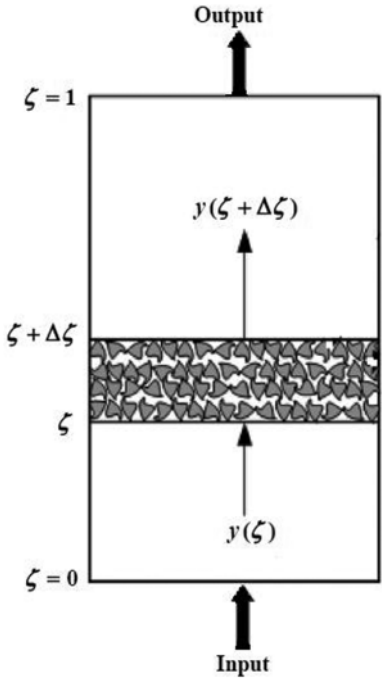

Fig. 2. Schematic diagram of the extraction bed.

2. Model Description

A schematic diagram of the extraction bed is presented in Fig. 2. Based on the assumptions, the dimensionless material balance differential equation in the mobile phase is derived as follows:

$$\frac{\partial y}{\partial \theta} + \tau_{int}\frac{\partial y}{\partial \zeta} = \frac{\tau_{int}}{Pe_b}\frac{\partial^2 y}{\partial \zeta^2} - 3Bi\left(\frac{1-\varepsilon_b}{\varepsilon_b}\right)(y - x_{\rho=1}) \quad (2)$$

where y and x are the dimensionless concentrations of solute in the bulk phase and inside the pores, respectively. Furthermore, ε_b is bed void fraction, while τ_{int}, Pe_b and Bi are dimensionless numbers (see nomenclature for details). Initial and boundary conditions are:

$$\text{IC: at } \theta=0, \text{ for all } \zeta,\ y=1 \quad (3)$$

$$\text{BC 1: at } \zeta=0, \text{ for all } \theta,\ y - \frac{1}{Pe_b}\frac{\partial y}{\partial \zeta} = 0 \quad (4)$$

$$\text{BC 2: at } \zeta=1, \text{ for all } \theta,\ \frac{\partial y}{\partial \zeta} = 0 \quad (5)$$

Assuming local equilibrium in the pores of the solid particles, the differential stationary phase mass balance is:

$$\left[\varepsilon_p + (1-\varepsilon_p)b\frac{\partial x_s}{\partial x}\right]\frac{\partial x}{\partial \theta} = \frac{1}{\rho^2}\frac{\partial}{\partial \rho}\left[\rho^2\frac{\partial x}{\partial \rho}\right] \quad (6)$$

where x_s is the dimensionless concentration of solute in the solid

phase. Furthermore ε_p is particle porosity and b is model constant (see nomenclature for details). The following Henry relationship was used between solute concentration in pore phase and solid part of particle:

$$c_s = Hc \rightarrow x_s = \frac{Hx}{b} \tag{7}$$

where c_s and c are solute concentration in the solid part and pore of seed, while H is Henry constant. By substitution of Eq. (7), Eq. (6) was converted into the following dimensionless form:

$$[\varepsilon_p + (1-\varepsilon_p)H]\frac{\partial x}{\partial \theta} = \frac{1}{\rho^2}\frac{\partial}{\partial \rho}\left[\rho^2 \frac{\partial x}{\partial \rho}\right] \tag{8}$$

The relevant dimensionless initial and boundary conditions are:

IC: at θ=0, for all ρ and ζ, x=1 (9)

BC 1: at ρ=0, for all ζ and θ, $\frac{\partial x}{\partial \rho} = 0$ (10)

BC 2: at ρ=1, for all ζ and θ, $\frac{\partial x}{\partial \rho} = Bi(y - x_{\rho=1})$ (11)

3. Numerical Solution

The explicit method of line was implemented to solve the partial differential Eqs. (2) and (8) and boundary conditions of (3-5) and (9-11). In this method, the length of extractor and the radius of the particles were divided into M (i=0, 1, …, M) and N parts (j=0, 1, …, N), respectively. Applying finite difference (central finite difference method), Eq. (2) is numerically converted as follows at (i=1, …, M−1):

$$\frac{\partial y_i}{\partial \theta} = \left(\frac{\tau_{int}}{2\Delta\zeta} + \frac{\tau_{int}}{Pe_b \Delta\zeta^2}\right) y_{i-1,n} + \left(\frac{-2\tau_{int}}{Pe_b \Delta\zeta^2} - 3Bi\left(\frac{1-\varepsilon_b}{\varepsilon_b}\right)\right) y_{i,n} + \left(\frac{-\tau_{int}}{2\Delta\zeta} + \frac{\tau_{int}}{Pe_b \Delta\zeta^2}\right) y_{i+1,n} + 3Bi\left(\frac{1-\varepsilon_b}{\varepsilon_b}\right) x_{N,i,n} \tag{12}$$

In Eq. (12), $y_{i,n}$ denotes the dimensionless concentration of solute in the mobile phase at $i\Delta\zeta$L and $n\Delta\theta = n(D_{eff}/R_p^2)\Delta t$. Accordingly, the finite difference form of initial and boundary conditions for this equation are:

IC: at θ=0(n=0), $y_{i,0}$=1, For (i=0, 1, …, M) (13)

BC 1: at ζ=0(i=0), $y_{0,n} - \frac{1}{Pe_b}\left[\frac{-3y_{0,n} + 4y_{1,n} - y_{2,n}}{2\Delta\zeta}\right] = 0$

$$y_{0,n} = \frac{1}{3 + 2Pe_b\Delta\zeta}(4y_{1,n} - y_{2,n}) \tag{14}$$

BC 2: at ζ=1(i=M), $\left[\frac{3y_{M,n} - 4y_{M-1,n} + y_{M-2,n}}{2\Delta\zeta}\right] = 0$

$$y_{M,n} = \left(\frac{4}{3}y_{M-1,n} - \frac{1}{3}y_{M-2,n}\right) \tag{15}$$

Applying finite difference to Eq. (8) results in the following Eq. at (i=0, 1, …, M) and (j=1, …, N−1):

$$\frac{\partial x_{j,i}}{\partial \theta} = \frac{1}{[\varepsilon_P + (1-\varepsilon_P)H]\Delta\rho^2}\left[\left(1 - \frac{1}{j}\right)x_{j-1,i,n} - 2x_{j,i,n} + \left(1 + \frac{1}{j}\right)x_{j+1,i,n}\right] \tag{16}$$

In Eq. (16), $x_{j,i,n}$ denotes the dimensionless concentration of solute at $i\Delta\zeta$L (from extraction column inlet), $j\Delta\rho R_p$ (from particle center) and $n\Delta\theta = n(D_{eff}/R_p^2)\Delta t$. The relevant initial and boundary conditions are:

IC: at θ=0(n=0), $x_{j,i,0}$=1, For (i=0, 1, …, M) and (j=0, 1, …, N) (17)

BC 1: at ρ=0(j=0), $\left[\frac{-3x_{0,i,n} + 4x_{1,i,n} - x_{2,i,n}}{2\Delta\rho}\right] = 0$

$$x_{0,i,n} = \left(\frac{4}{3}x_{1,i,n} - \frac{1}{3}x_{2,i,n}\right), \text{ For (i=0, 1, …, M)} \tag{18}$$

BC 2: at ρ=1(j=N), $\left[\frac{3x_{N,i,n} - 4x_{N-1,i,n} + x_{N-2,i,n}}{2\Delta\rho}\right] = Bi(y_{i,n} - x_{N,i,n})$

$$x_{N,i,n} = \frac{1}{3 + 2Bi\Delta\rho}(4x_{N-1,i,n} - x_{N-2,i,n} + 2Bi\Delta\rho y_{i,n}),$$

For (i=0, 1, …, M) (19)

The set of ODEs (12,16) obtained using the central finite difference method was solved via explicit method of line. The experimental data of oil extraction recovery was used for the modeling validation and this quantity is theoretically defined in Eq. (20).

$$F(\theta) = \frac{\varepsilon_b \tau_{int}}{[\varepsilon_p + (1-\varepsilon_p)H](1-\varepsilon_b)}\int_0^{\theta} y_{\xi=1}\, d\theta \tag{20}$$

4. Estimation of Model Parameters

The density of supercritical carbon dioxide was obtained from IUPAC data [23]. The viscosity of pure CO_2 was estimated as a function of the reduced temperature ($T_r = T/T_c$), reduced density ($\rho_{fr} = \rho_f/\rho_{fc}$) and low-pressure gas viscosity (μ_f^0) using the method of Jossi et al. [24] for nonpolar gases. The physical properties of SC-CO_2 under various operating conditions are shown in Table 1. The bed porosity of the packed column was measured to be 0.5 and the particle porosity was evaluated via the nitrogen desorption technique to be 0.12.

Molecular diffusion coefficient (D_{AB}) was obtained using Chao-Hong He correlation [25]. The dominant fatty acid in the *E. amoenum* seed oil is α-linolenic acid (ALA) (40-41% as shown in Table 2). Thus the physical properties of ALA were used in calculation of molecular diffusion coefficient. The Eq. for the effective diffusivity in the particle was given by Wakao and Smith [26]:

Table 1. Experimental conditions and physical properties of SC-CO_2

Run	T (K)	P (MPa)	Q (ml/min)	ρ_f (kg/m^3)	μ_f ($\times 10^{-5}$ Kg/m s)
1	313	25	1.2	880	8.10
2	318	25	1.2	858	7.75
3	323	25	1.2	835	7.41
4	328	25	1.2	811	7.08
5	323	15	1.2	701	5.72
6	323	20	1.2	785	6.71
7	323	30	1.2	871	7.99
8	323	25	0.6	835	7.41
9	323	25	0.9	835	7.41
10	323	25	1.5	835	7.41

Table 2. Fatty acid composition of *E. amoenum* seed oil: comparison of SFE and Soxhlet extraction

Fatty acids	Extraction method	
	Soxhlet (wt%)	SFE (wt%)
Palmitic acid, C16:0	6.5	6.8
Stearic acid, C18:0	3.9	3.4
Oleic acid, C18:1 (n-9)	13.2	13.3
Linoleic acid, C18:2 (n-6)	20.1	19.5
γ-Linolenic acid, C18:3 (n-6)	7.1	7.3
α-Linolenic acid, C18:3 (n-3)	40.3	40.7
Stearidonic acid, C18:4 (n-3)	8.9	9.0
MUFA	13.2	13.3
PUFA	76.4	76.5
UFA	89.6	89.8
SFA	10.4	10.2

$$D_{eff}=\varepsilon_p^2 D_{AB} \quad (21)$$

The supercritical fluid film mass transfer coefficient was estimated using the empirical correlation reported by Tan et al. as below [27]:

$$Sh=0.38Re^{0.83}Sc^{1/3},\ 2<Re<40,\ 2<Sc<20 \quad (22)$$

Axial dispersion coefficient was calculated via correlation of Funazukuri et al. as below [28]:

$$\frac{\varepsilon_b D_{ax}}{D_{AB}}=1.317(ReSc)^{1.392},\ ReSc>0.3 \quad (23)$$

Moreover, the Henry constant used in the modeling of this study was estimated via GA.

5. Genetic Algorithm Application in Estimation of Henry Constant

Genetic algorithm is an appropriate method for parameter estimation. Genetic algorithm is a search procedure based on the concepts of natural selection, genetics and evolution (Darwinian survival), usually utilized for both its accuracy and global searching ability in the optimization problems of different engineering disciplines [29, 30]. Genetic algorithm does not need initial guesses in contrast to the ordinary optimization methods.

We applied GA to determine the optimal value of the Henry constant such that to minimize the absolute average deviations (AAD) between the experimental and predicted extraction recoveries. The AAD was calculated according to Eq. (24):

$$AAD\% = \frac{1}{NP}\sum_{i=1}^{NP}\left|\frac{F_{exp,i}-F_{mod\,el,i}}{F_{exp,i}}\right|\times 100 \quad (24)$$

where NP is the number of data points. The procedure is:

1. Define the objective function according to Eq. (24).
2. Characterization of GA parameters (population size: 35, generations: 100, selection method: tournament, elite count: 2, crossover method: two point crossover, crossover fraction: 0.6 and mutation method: Gaussian).
3. Production of initial generation in a random way.
4. Fitness evaluation.
5. Production of a new generation using the GA operators (selection, crossover and mutation).

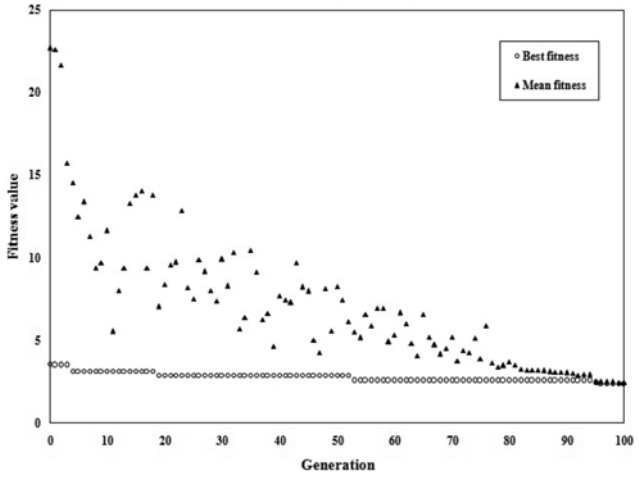

Fig. 3. Variation of fitness function *versus* generation at T=313 K, P=25 MPa and Q=1.2 ml/min.

6. Repeat steps 4-5 until the number of generation reaches the prescribed value.

The variation of fitness value *versus* generation is shown in Fig. 3. As demonstrated in this figure, the mean fitness gradually reaches the best fitness as a function of generation progress and finally coincides with best fitness at the generation of approximately 95.

RESULTS AND DISCUSSION

1. Fatty Acid Composition of Extracted Oil

The SC-CO_2 extraction of essential oil from *E. amoenum* seed was carried out utilizing different operating conditions of ten experimental runs shown in Table 1. The GC-FID chromatogram of fatty acids (from *E. amoenum* seed oil) extracted by supercritical CO_2 at 25 MPa, 318 K with CO_2 flow rate of 1.2 ml/min and dynamic time of 160 min is presented in Fig. 4. Table 2 presents the fatty acid composition of the extracted oil by SC-CO_2 at the same operating conditions of Fig. 4 and its comparison with the conventional Soxhlet method. Not much difference is observed in the fatty acid composition of the extracted oil by the two methods. Table 2 shows that the fatty acids in the *E. amoenum* seed oil were dominated by polyunsaturated fatty acids (PUFA), which accounted for more than 76% of the total fatty acids. Monounsaturated fatty acids (MUFA) were the second most abundant at approximately 13% while the content

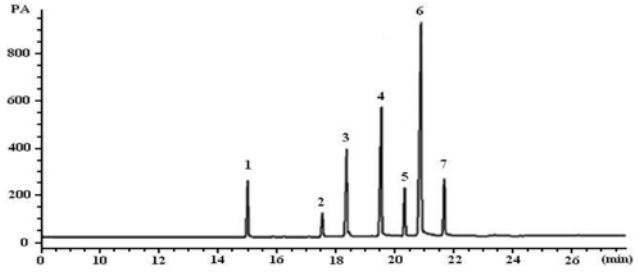

Fig. 4. GC-FID chromatogram of FAMEs at T=318 K, P=25 MPa, Q=1.2 ml/min and dynamic time of 160 min. Detected peaks. 1=C16:0, 2=C18:0, 3=C18:1 (n-9), 4=C18:2 (n-6), 5=C18:3 (n-6), 6=C18:3 (n-3), 7=C18:4 (n-3)

Table 3. Mass transfer parameters and absolute average deviations

T (K)	P (MPa)	Q (ml/min)	D_{eff} ($\times 10^{-10}$ m^2/s)	H	k_f ($\times 10^{-5}$ m/s)	D_{ax} ($\times 10^{-6}$ m^2/s)	AAD%
313	25	1.2	0.83	0.25	1.28	2.96	2.38
318	25	1.2	0.88	0.22	1.35	2.89	1.71
323	25	1.2	0.94	0.24	1.42	2.81	3.03
328	25	1.2	1.01	0.28	1.50	2.74	4.14
323	15	1.2	1.27	0.47	1.81	2.51	4.00
323	20	1.2	1.05	0.31	1.56	2.70	3.72
323	30	1.2	0.87	0.21	1.33	2.90	2.52
323	25	0.6	0.94	0.24	0.80	1.07	4.04
323	25	0.9	0.94	0.24	1.12	1.89	2.52
323	25	1.5	0.94	0.24	1.71	3.84	1.73

of saturated fatty acids (SFA) was less than 11% of the total fatty acids. The main PUFA in the *E. amoenum* seed oil were α-linolenic acid (ALA) (40-41%), followed by linoleic acid (LA) (19-20%). The aforementioned results were expressed in GC area% based on separation via GC-FID capillary column. Seed fatty acid profiles obtained in this study are in close agreement with previous investigations [31]. For instance, the results of this study indicated high amount of ALA (40-41%) in *Echium* species which is confirmed by the previous reports [31,32].

2. Model Validation

To investigate the authenticity of the developed model, the experimental measurements of supercritical extraction of essential oil from *E. amoenum* seed were compared with the modeling predictions for the extraction recovery. The calculated AAD% for extraction recovery in conjunction with the mass transfer parameters is shown in Table 3. It is clear that the observed deviations are less than 5% for all operating conditions, which is an indication of a very good compatibility and validation for the developed model.

3. Effect of Temperature

Fig. 5 shows the effect of temperature on the modeling extraction recovery (demonstrated as continuous line) at the operating conditions of 25 MPa and 1.2 ml/min and its comparison with the experimental measurements (shown as individual data points). On one hand, increasing the temperature results in a decrease in the SC-CO_2 density and its solubility power, while on the other hand, it leads to an increase in the vapor pressure of solute and higher diffusivity and mass transfer coefficient. In this study, the results show that increasing the extraction temperature, from 313 to 318 K, favors the extraction recovery because of increasing the vapor pressure of essential oil, while higher temperature lowers down the recovery because of decreasing the solvent density. This counter-effect phenomenon is called retrograde solubility in which supercritical fluid density and solute vapor pressure are function of temperature in an opposite trend. Therefore, it is mandatory to locate an optimal operating temperature to achieve the maximum recovery. The modeling predictions of Fig. 5 demonstrate a very close compatibility for the maximum recovery (77.1%) with the experimental results (76.1%) at 318 K and 160 min.

4. Effect of Pressure

As shown in Fig. 6, the modeling predictive recovery (demonstrated as continuous line) of essential oil *versus* dynamic time is plotted for four different pressures at constant 323 K and 1.2 ml/min

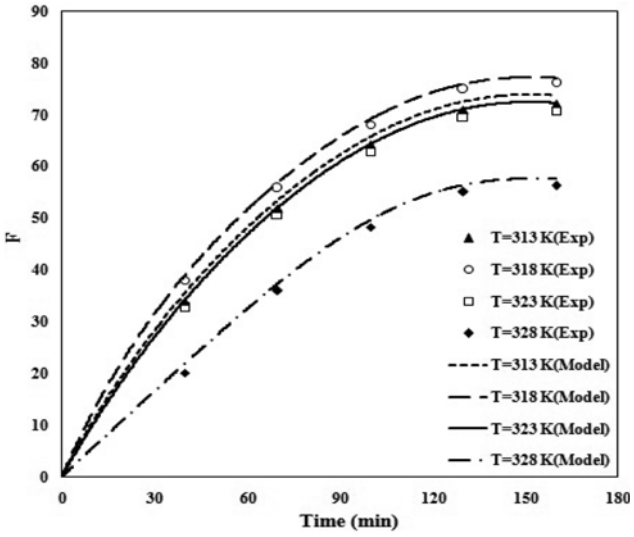

Fig. 5. Effect of temperature on essential oil recovery at P=25 MPa and Q=1.2 ml/min.

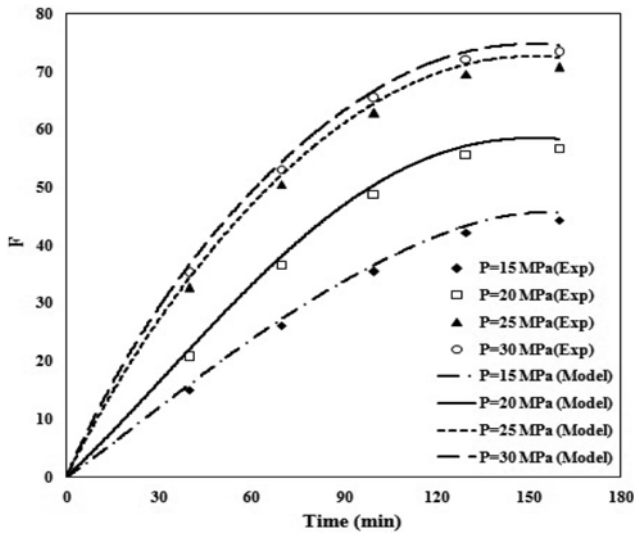

Fig. 6. Effect of pressure on essential oil recovery at T=323 K and Q=1.2 ml/min.

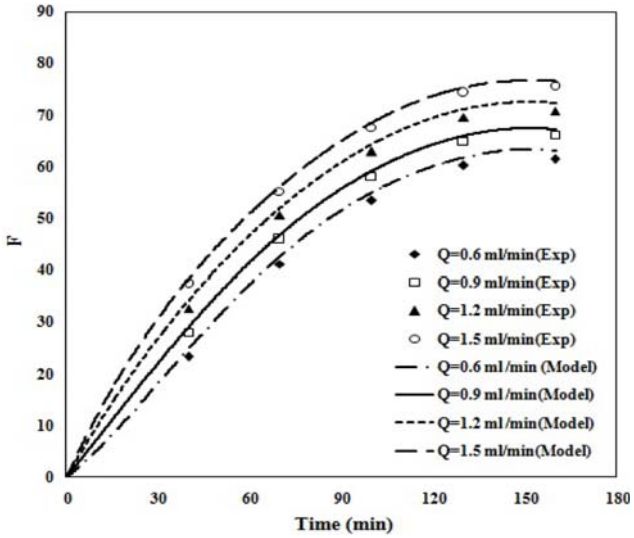

Fig. 7. Effect of flow rate on essential oil recovery at T=323 K and P=25 MPa.

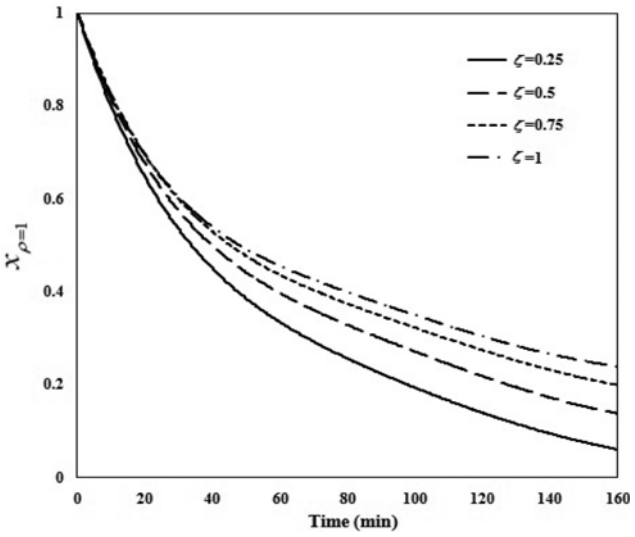

Fig. 8. Variation of solute concentration in pore phase along the SFE bed at T=313 K, P=25 MPa and Q=1.2 ml/min.

and compared with experimental results (shown as individual data points). A very close compatibility is observed between the predictive and experimental data for all the considered operating conditions. As far as the recovery trend as a function of pressure is concerned, the extraction recovery of essential oil significantly increased with increasing pressure, especially in the operating range of 15-25 MPa. The recovery at dynamic time of 160 min enhanced 58.8% when the pressure increased from 15 to 25 MPa. The change of extraction recovery *versus* pressure is due to a dual effect. On one hand, increasing the pressure causes higher SC-CO_2 density, and therefore, improves the solubility of solute and leads to higher recovery. On the other hand, increasing the pressure reduces the solute diffusivity and mass transfer coefficient, resulting in a lower enhancement trend of the recovery [33]. This phenomenon is observed when the pressure is raised from 25 to 30 MPa.

5. Effect of SC-CO_2 Flow Rate

The effect of CO_2 flow rate on the oil recovery is presented in Fig. 7 via modeling (demonstrated as continuous line) and experimental data (shown as individual data points) at constant 323 K and 25 MPa. Again, similar to two previous diagrams, a very close compatibility is observed between the predictive and experimental recovery for all the considered operating conditions. The CO_2 flow rate exhibited a positive and significant effect on the *E. amoenum* seed oil recovery. The recovery enhanced 21.3% when the flow rate increased from 0.6 to 1.5 ml/min. This enhancement trend might be due to the decrease in the mass transfer resistance with increasing flow rate. In other words, higher SC-CO_2 velocity decreases supercritical fluid film thickness around the stationary phase (*E. amoenum* seed), which subsequently lowers the exterior mass transfer resistance.

6. Effect of Dynamic Extraction Time

As shown in Figs. 5-7, it is obvious that the extraction recovery increases with increasing extraction time. Similarly, according to Fig. 8 (solute concentration in pore phase at solid surface ($x_{\rho=1}$) *versus* time at different axial position of the extraction column), the recovery profile does not have a constant trend because the solute desorption rate from the solid phase deceases with increasing time. In other words, as demonstrated in Fig. 8, at the beginning a sharp decreasing slope in the desorption concentration profile is observed and subsequently the trend in the profile decreases. These two distinguished trends may be explained in terms of the existence of a very high mass transfer driving force in the first 90 min and subsequently gradual depletion of essential oil in the stationary phase causes a moderate decreasing slope at higher dynamic time (>90 min). The two observed trends in Figs. 5-8 indicate that it is necessary to approximately pinpoint an optimal dynamic extraction time in which a very high extraction rate (mass transfer driving force) leads to high amount of extraction in a short period of time. Obviously, lower operating costs in terms of the amount of used supercritical fluid and electricity will be achieved via the application of appropriate operating conditions. Accordingly, it seems that an optimal dynamic time can be selected at about 90 min with the implementation of a CO_2 recycle stream for the extraction of the remaining essential oil.

CONCLUSIONS

We did a parametric analysis (pressure, temperature, flow rate of supercritical carbon dioxide and dynamic extraction time) of essential oil extraction from *E. amoenum* seed using supercritical carbon dioxide via a validated mathematical model. Adjustable parameter of the Henry constant was estimated by fitting the experimental and modeling data using genetic algorithm technique. Temperature had a complex effect on essential oil recovery and showed a maximum at 318 K. Increase in pressure from 15 to 30 MPa enhanced the recovery due to increase in density. Increase of CO_2 flow rate from 0.6 to 1.5 ml/min caused enhancement in the essential oil recovery due to higher mass transfer coefficient. Overall, it can be concluded via the obtained experimental and modeling data that supercritical fluid technology is a viable technique for extraction of very valuable products from natural plant resources. The experimental and modeling results of this research can be implemented in pinpointing a set of optimum operating conditions to achieve the maximum oil recovery.

ACKNOWLEDGEMENT

The financial support provided for this project by Isfahan University of Technology (IUT) is gratefully acknowledged.

NOMENCLATURE

b : model constant, c_{s0}/c_0
Bi : Biot number, $k_f R_p/D_{eff}$
c : solute concentration in the pore of *E. amoenum* seed [kmol/m^3]
c_0 : solute concentration in the pore of *E. amoenum* seed at t=0 [kmol/m^3]
c_s : solute concentration in the solid part of *E. amoenum* seed [kmol/m^3]
c_{s0} : solute concentration in the solid part of *E. amoenum* seed at t=0 [kmol/m^3]
C : solute concentration in the supercritical phase [kmol/m^3]
D_{AB} : molecular diffusion coefficient [m^2/s]
D_{ax} : axial dispersion coefficient [m^2/s]
D_{eff} : effective pore diffusivity [m^2/s]
F : recovery of essential oil
H : Henry constant
k_f : mass transfer coefficient [m/s]
L : bed length [m]
M : column axial discrete subdivision
N : solid particle radial discrete subdivision
P : pressure [MPa]
Pe_b : Peclet number for the bed, uL/D_{ax}
Q : SC-CO_2 flow rate [ml/min]
r : radial distance coordinate in particle [m]
R_p : particle radius [m]
Re : Reynolds number, $2R_p\varepsilon_b u\rho_f/\mu_f$
Sc : Schmidt number, $\mu_f/\rho_f D_{AB}$
Sh : Sherwood number, $2R_p k_f/D_{AB}$
t : time [s]
T : temperature [K]
T_c : critical temperature [K]
T_r : reduced temperature, T/T_c
u : interstitial fluid velocity [m/s]
x : dimensionless concentration in pore phase, c/c_0
x_s : dimensionless concentration in solid phase, c_s/c_{s0}
y : dimensionless concentration in bulk phase, C/c_0
z : axial distance [m]

Greek Letters

$\Delta\theta$: dimensionless time increment
$\Delta\rho$: dimensionless length of radial coordinate increment, 1/N
$\Delta\zeta$: dimensionless length of axial coordinate increment, 1/M
ε_b : bed void fraction
ε_p : particle porosity
μ_f : viscosity of SC-CO_2 [kg/m s]
μ_f^0 : low-pressure gas viscosity [kg/m s]
θ : dimensionless time, tD_{eff}/R_p^2
ρ : dimensionless radial coordinate in particle, r/R_p
ρ_f : density of SC-CO_2 [kg/m^3]
ρ_{fc} : critical density of CO_2 [kg/m^3]
ρ_{fr} : reduced density of SC-CO_2, ρ_f/ρ_{fc}
ζ : dimensionless axial distance, z/L
τ_{int} : internally controlled, characteristic extraction time, $uR_p^2/(LD_{eff})$

Subscripts

b : bed
c : critical
f : fluid
p : particle
s : solid
0 : at time zero

Abbreviations

AAD : absolute average deviation
ALA : α-linolenic acid
FAME : fatty acid methyl ester
GA : genetic algorithm
GLA : γ-linolenic acid
I.D. : inner diameter
LA : linoleic acid
MUFA : monounsaturated fatty acids
PUFA : polyunsaturated fatty acids
SC-CO_2 : supercritical carbon dioxide
SDA : stearidonic acid
SFA : saturated fatty acids
SFE : supercritical fluid extraction

REFERENCES

1. B. Shafaghi, N. Naderi, L. Tahmasb and M. Kamalinejad, *Iran J. Pharm. Res*., **1**, 1 (2002).
2. J. A. Menendez, R. Colomer and R. Lupu, *Med. Hypo. Theses*, **64**, 2 (2005).
3. H. Ge, X. Kong, L. Shi, L. Hou, Z. Liu and P. Li, *Cell Biol. Int.*, **33**, 3 (2009).
4. L. Wang, C. L. Weller, V. L. Schlegel, T. P. Carr and S. L. Cuppett, *Bioresour. Technol.*, **99**, 5 (2008).
5. S. Lucas, M. P. Calvo, J. Garcia-Serna, C. Palencia and M. J. Cocero, *J. Supercrit. Fluids*, **41**, 2 (2007).
6. E. L. G. Oliveira, A. J. D. Silvestre and C. M. Silva, *Chem. Eng. Res. Des.*, **89**, 1104 (2011).
7. Z. Huang, X. H. Shi and W. J. Jiang, *J. Chromatogr. A*, **1250**, 2 (2012).
8. M. G. Bernardo-Gil and M. Casquilho, *AIChE J.*, **53**, 11 (2007).
9. D. Mongkholkhajornsilp, S. Douglas, P. L. Douglas, A. Elkamel, W. Teppaitoon and S. Pongamphai, *J. Food Eng.*, **71**, 4 (2005).
10. F. Gaspar, T. Lu, R. Santos and B. Al-Duri, *J. Supercrit. Fluids*, **25**, 3 (2003).
11. E. Reverchon and L. Sesti Osseo, *Chem. Biochem. Eng. Q.*, **8**, 1 (1994).
12. U. Salgin, Döker and A. ÇalImlI, *J. Supercrit. Fluids*, **38**, 3 (2006).
13. A. K. K. Lee, N. R. Bulley, M. Fattori and A. Meisen, *J. Am. Oil Chem. Soc.*, **63**, 7 (1986).
14. E. Reverchon and C. Marrone, *Chem. Eng. Sci.*, **52**, 20 (1997).
15. E. Reverchon and M. Poletto, *Chem. Eng. Sci.*, **51**, 15 (1996).
16. E. M. C. Reis-Vasco, J. A. P. Coelho, A. M. F. Palavra, C. Marrone and E. Reverchon, *Chem. Eng. Sci.*, **55**, 15 (2000).

17. S. M. Ghoreishi, R. G. Shahrestani and H. S. Ghaziaskar, *Chem. Eng. Technol.*, **32**, 1 (2009).
18. H. Sovová, J. Kuera and J. Je, *Chem. Eng. Sci.*, **49**, 3 (1994).
19. J. Stastova, J. Jez, M. Bartlova and H. Sovova, *Chem. Eng. Sci.*, **51**, 18 (1996).
20. C. Marrone, M. Poletto, E. Reverchon and A. Stassi, *Chem. Eng. Sci.*, **53**, 21 (1998).
21. E. Reverchon, J. Daghero, C. Marrone, M. Mattea and M. Poletto, *Ind. Eng. Chem. Res.*, **38**, 8 (1999).
22. H. J. Kim, S. B. Lee, K. A. Park and I. K. Hong, *Sep. Purif. Technol.*, **15**, 1 (1999).
23. S. Angus, B. Armstrong and K. M. De-Reuck, *IUPAC: International thermodynamics tables of the fluid state carbon dioxide*, Pergamon Press, New York (1976).
24. B. E. Poling, J. M. Prausnitz, O. C. John Paul and R. C. Reid, *The properties of gases and liquids*, McGraw-Hill, New York (2001).
25. C. H. He, Y. S. Yu and W. K. Su, *Fluid Phase Equilib.*, **142**, 1 (1998).
26. N. Wakao and J. M. Smith, *Chem. Eng. Sci.*, **17**, 11 (1962).
27. C. S. Tan, S. K. Liang and D. C. Liou, *Chem. Eng. J.*, **38**, 1 (1988).
28. T. Funazukuri, C. Kong and S. Kagei, *J. Supercrit. Fluids*, **13**, 1 (1998).
29. D. E. Goldberg, *Genetic algorithms in search, optimization and machine learning*, Addision Wesley, MA (1989).
30. J. H. Holland, *Adaptation in natural and artificial systems*, MIT Press Cambridge, MA (1992).
31. J. L. Guil-Guerrero, J. C. López-Martínez, F. Gómez-Mercado and P. Campra-Madrid, *Eur. J. Lipid Sci. Technol.*, **108**, 1 (2006).
32. E. Daukas, P. R. Venskutonis and B. Sivik, *J. Supercrit. Fluids*, **22**, 3 (2002).
33. A. Salimi, S. Fatemi, H. Z. N. Nei and A. Safaralie, *Chem. Eng. Technol.*, **31**, 10 (2008).